Thermochimica Acta, 145 (1989) 115–130
Elsevier Science Publishers B.V., Amsterdam – Printed in The Netherlands

THE EFFECT OF EXPERIMENTAL VARIABLES ON THE MECHANISM OF THE OXIDATION OF PYRITE. PART 1. OXIDATION OF PARTICLES LESS THAN 45 μm IN SIZE

J.G. DUNN and G.C. DE

School of Applied Chemistry, Curtin University of Technology, Perth (Australia)

B.H. O'CONNOR

School of Physics and Geosciences, Curtin University of Technology, Perth (Australia)

(Received 9 August 1988)

ABSTRACT

The oxidation of pyrite of particle size less than 45 μm has been studied by simultaneous thermogravimetry–differential thermal analysis (TG–DTA) at a heating rate of 2.5 °C min^{-1} in an air atmosphere. Sample masses of approximately 1.8 mg were contained in platinum crucibles. Partially oxidised samples were isolated and the phase composition determined by quantitative X-ray diffraction (XRD). Micrographs of these samples were obtained by scanning electron microscopy (SEM). Four effects were observed in the DTA record. At temperatures of 395–420 °C there were several sharp exotherms. XRD analysis showed the presence of 90% pyrite and 6% hematite in samples heated to 428 °C. Beyond this there was a broad exotherm, with a shoulder on the high temperature side, in the temperature range 420–490 °C. By 470 °C, 47% hematite was detected with 36% pyrite remaining. By 505 °C 65% hematite was present with 10% pyrite unreacted. Beyond this temperature there was a weak endotherm which was complete by 610 °C. Only hematite was detected in a sample heated to 696 °C. The corresponding TG curves showed two major weight losses, the first in the temperature range 440–480 °C and the second between 550–605 °C. The SEM results indicated that reacted particles had little general porosity. Increasing the heating rate progressively from 2.5 to 40 °C min^{-1} caused a significant change in the TG–DTA curve, with a decrease in the intensity of the major exothermic peak, and the appearance of a new peak between 530–550 °C. The second weight loss decreased relative to the first weight loss. Changing the atmosphere from air to oxygen and heating at 40 °C min^{-1} produced a further significant change in the TG–DTA record. Only one intense exotherm and one rapid weight loss were observed between 475–500 °C. The particles, when examined by SEM, had a very high porosity. The differences in appearance of the TG–DTA records have been attributed to changes in the reaction mechanism which occur as a result of variation in the experimental conditions.

INTRODUCTION

The oxidation of pyrite has been extensively studied by thermal analysis techniques. There is general agreement that the final product is hematite. However, various pathways to this end product have been proposed.

0040-6031/89/$03.50

The simplest reaction pathway involves the direct oxidation of pyrite to hematite. The formation of hematite by this reaction has been confirmed by petrographic analysis at temperatures above 325 °C [1] and by XRD at 370–480 °C [2].

A second pathway involves the formation of hematite by the thermal decomposition of iron(II) sulphate ($FeSO_4$). In isothermal TG studies, the latter has been reported at temperatures as low as 100 °C, with a maximum rate of formation at 200 °C [1]. $FeSO_4$ commenced decomposition above 225 °C, and was not detected above 320 °C [1], although some workers have reported it present at temperatures of 460–480 °C [3]. Further oxidation of $FeSO_4$ is reported to produce $[Fe_2(SO_4)_3]_2 \cdot Fe_2O_3$ [3].

Another mechanism involves pyrrhotite formation as an intermediate step. However, only one report has provided supporting evidence to justify this suggestion [4]. Using microprobe analysis and quantitative SEM, Jorgensen and Moyle [4] observed an outer layer of initial oxide, a thick layer of porous oxide and a core of unreacted pyrite. A small amount of pyrrhotite was present at the interface between the pyrite core and the porous oxide layer. This phase was only observed in the temperature range 530–550 °C.

Finally, it has been suggested that hematite is formed by the reaction of an iron(III) sulphate species. Two possible routes, either through interaction between unreacted pyrite and sulphate [5,6], or thermal decomposition of the sulphate [3,7] have been proposed. Such reactions tend to occur at relatively high temperatures, so that the decomposition of the reported intermediate $Fe_2(SO_4)_3$ [5] occurs above 550 °C [3].

The studies documented in the literature have primarily been carried out over a limited range of experimental variables, for example at heating rates of 10 °C min^{-1}, and particle sizes (where reported) of 50–80 μm. We have investigated the oxidation of pyrite over a much wider set of experimental conditions, which include variation in the particle size, heating rate and oxygen concentration. This paper reports on the oxidation of particles of less than 45 μm. The oxidation of particles between 90 and 125 μm will be reported in a subsequent publication.

EXPERIMENTAL

Materials

The pyrite used in the present study was a natural product from the Dominican Republic. Electron probe microanalysis (EPMA) and chemical analysis determined the major elements to be Fe (46.1%) and S (52.8%) so that the impurity content was approximately 1.1%. Energy dispersive X-ray analysis on the SEM indicated the presence of Ti, Si, Al, Ca, K and Cl as

impurities. Finally the mineral form of the Dominican pyrite was confirmed by XRD.

Air and oxygen were of industrial grade and obtained from The Commonwealth Industrial Gases Ltd.

Thermal analysis

A quantity (≈ 5 g) of the Dominican pyrite was hand ground in an agate mortar and pestle. This material was then sieved through Brass Endecott Laboratory Test Sieves to isolate the < 45 μm fraction.

Simultaneous TG–DTA measurements were performed using a Stanton Redcroft Model 780 Thermal Analyser interfaced to an IBM microcomputer. The platinum sample crucibles were 5.2 mm in internal diameter and 4.0 mm in height.

Approximately 1.8 mg of the sample was weighed into a platinum crucible, spread as far as possible as a monolayer, and placed in the TG–DTA apparatus. A gas flow of 30 ml min^{-1} was established. The temperature programme was started at ambient temperature and completed at 800 °C.

X-Ray diffraction

For quantitative analysis, about 2.00 mg of the sample was taken in a small agate mortar and ground carefully for 10 min to produce optimum particle size (< 10 μm). A weighed amount of the fine powder thus prepared was taken, suspended in petroleum ether, (b.p. 60–80 °C) using an ultrasonic bath and then filtered onto a Millipore type AA filter paper (pore size 0.80 μm, diameter 13 mm). A thin sample prepared in this way was fixed to a plastic sample holder with double-sided adhesive tape.

XRD patterns were acquired using a Siemens type-E powder diffractometer fitted with a copper X-ray tube, rotating specimen stage and a sealed Xe-gas proportional detector. The X-ray tube was operated at 45 kV and 16 mA. Patterns were recorded with Cu $K\alpha$ ($\lambda = 1.5418$ Å) radiation by using a nickel filter to suppress the Cu $K\beta$ component.

The sample was mounted on the diffractometer, and scanned using the following typical instrument settings

Goniometer speed	$1°$ min^{-1}
Sensitivity range	1×10^3 counts s^{-1}
Time constant	10 s for quantitative analysis
Chart speed	1 cm min^{-1}
Detector angle range	6–96 °
Detector voltage	2 kV
Amplifier gain	20
Pulse height setting	lower level 1 V
	window 2 V

Scanning electron microscopy

Samples were mounted in epoxy resin, polished and gold coated. SEM was performed using a JEOL JSM-35C scanning electron microscope fitted with a secondary electron, a backscattered electron and an X-ray energy dispersive (e.g. Si(Li)) detector. A tungsten filament was used as the source of primary electrons which were accelerated to 25 keV energy. X-Ray energy spectra were obtained using a TN-1705 multichannel analyser and copies were produced with an X–Y plotter. Photographs were taken using a 665 Polaroid camera.

RESULTS AND DISCUSSION

The pyrite sample was oxidised under a variety of experimental conditions. Three sets of experiments were conducted which involved:

(a) heating the samples in air at 2.5 °C min^{-1} and examining the products at various stages of oxidation by XRD and SEM;

(b) changing the heating rate between 2.5 and 40 °C min^{-1};

(c) changing the atmosphere from air to oxygen.

Pyrite heated in air at 2.5 °C min^{-1}

Thermal analysis

A typical TG–DTA curve for the oxidation of pyrite under the above conditions is shown in Fig. 1. A two-stage weight loss is observed in the TG curve. The first weight loss had extrapolated onset and offset temperatures of 440 and 480 °C respectively. In the DTA record a number of sharp exotherms were visible between 395 and 420 °C, prior to a major exotherm between 420 and 490 °C. The second weight loss occurred in the temperature range 550–605 °C, and was associated with an endotherm occurring between 550 and 610 °C.

The first weight loss in the TG curve corresponds to the oxidation of pyrite to hematite [2,5,8,9] whilst the second weight loss and endothermic effect is attributed to the decomposition of an iron sulphate phase [3,7].

XRD

To establish the reaction sequences for the oxidation of pyrite at elevated temperatures, phase analysis was performed using XRD. Both qualitative and quantitative procedures were used. Samples were heated at 2.5 °C min^{-1} in an air atmosphere in the temperature range from ambient to around 700 °C. The reactions were stopped at certain selected temperatures as shown in Fig. 1 and the products examined.

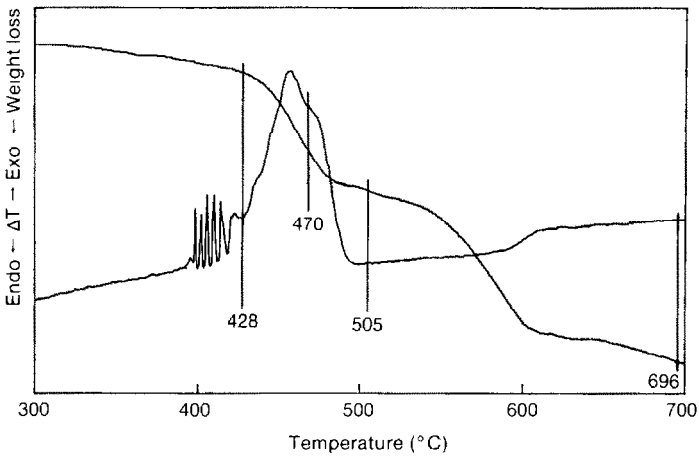

Fig. 1. TG–DTA trace of < 45 μm particles of pyrite heated at 2.5 °C min^{-1} in air. Temperatures at which oxidised samples were obtained for analysis are indicated by vertical lines.

The phases pyrite and hematite accounted for all lines in the XRD patterns. Any other species present were at too low a level to be detected or were amorphous.

To determine the percentage composition of the mixture of phases formed during oxidation, quantitative analysis was performed using a thin film method for which absorption corrections were negligible [10]. Diffraction intensities were therefore proportional to the mass of each analyte. Diffracted intensities corresponding to the two most intense lines for each phase were measured. The amount of pyrite and hematite present in the test samples heated to 428, 470, 505 and 696 °C (see Fig. 1) was estimated using calibration curves prepared with single-phase specimens. The results are presented in Table 1. It is evident from Table 1 that conversion of pyrite to hematite is the main reaction. However, the increasing deficit with temperature between the sum of the two detected phases and 100% indicates that at

TABLE 1

Weight percent of the phases measured by XRD during oxidation of pyrite (< 45 μm size fraction) at elevated temperatures

Sample temperature (°C)	Phase composition (%)		Deficit (%)
	Pyrite	Hematite	
428	90 ± 3	6 ± 5	4 ± 8
470	36 ± 4	47 ± 7	17 ± 11
505	10 ± 2	65 ± 4	25 ± 6
696	[a]	100 ± 3	0

[a] Not detected.

least one more reaction is taking place simultaneously. There were no unassigned lines in the diffraction patterns even though the phase or phases formed were present at the 25% level.

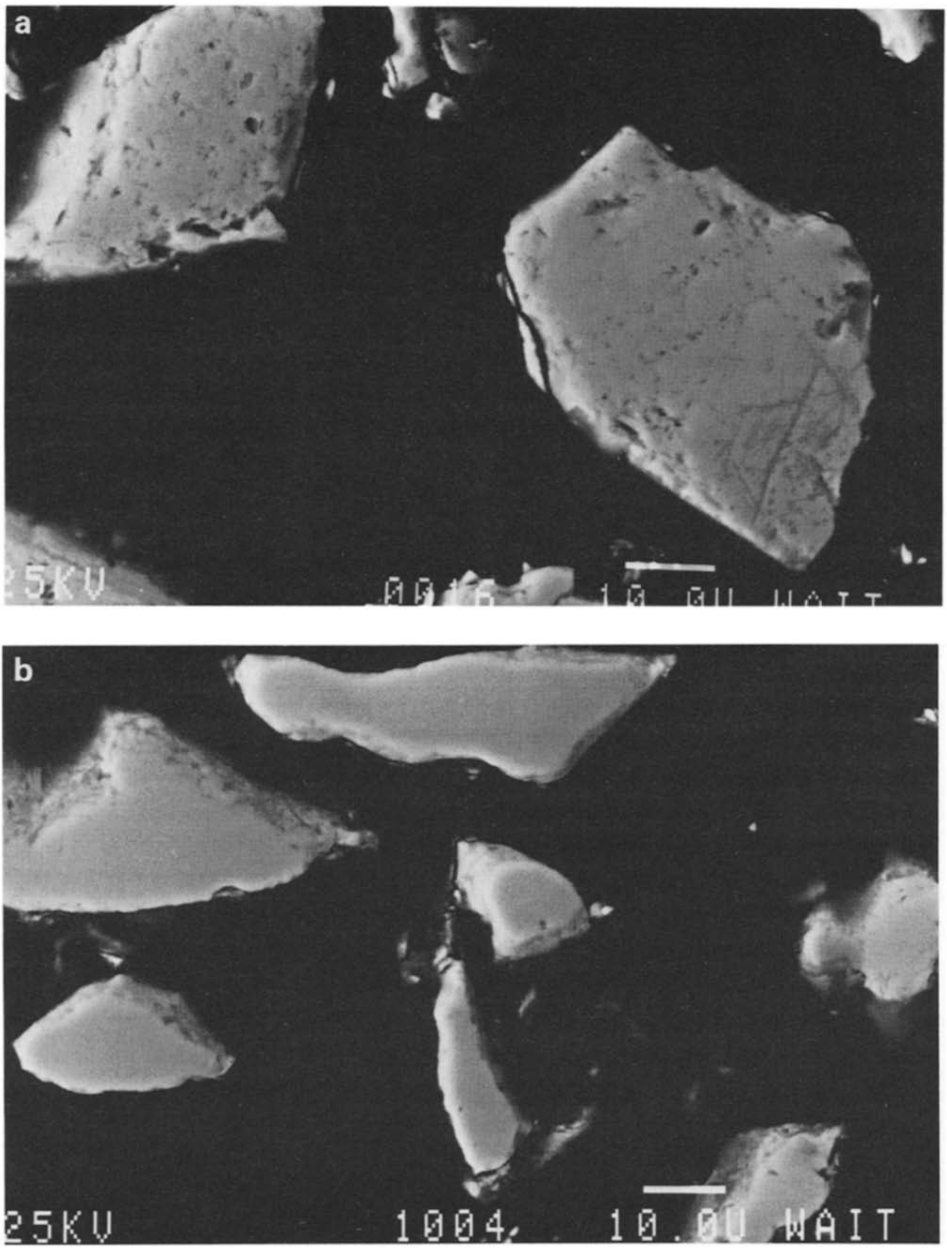

Fig. 2. Scanning electron micrographs of $< 45\ \mu m$ particles of pyrite heated at 2.5 °C min^{-1} in air to various temperatures and then cooled rapidly to room temperature: (a) unreacted pyrite, (b) 30–428 °C, (c) 30–470 °C, (d) 30–505 °C, (e) 30–696 °C.

SEM

To examine the behaviour of individual particles at elevated temperatures towards oxidising conditions, further samples were prepared under the same conditions as those for XRD (see Fig. 1).

SEM micrographs of representative particles are shown in Fig. 2. Figure 2a represents unreacted pyrite particles. In general, the particle surface is smooth with a metallic lustre. In some cases, particles also contain cavities or inclusions. A comparison of the micrographs of the unreacted pyrite particles with those of the partially or completely reacted particles reveals that no observable change occurs for particles heated to 428 °C (Fig. 2b). However, the particles heated to 470 °C have undergone a significant extent of oxidation (Fig. 2c). Generally the smaller particles are observed to react completely by this temperature whilst the larger ones have partially reacted.

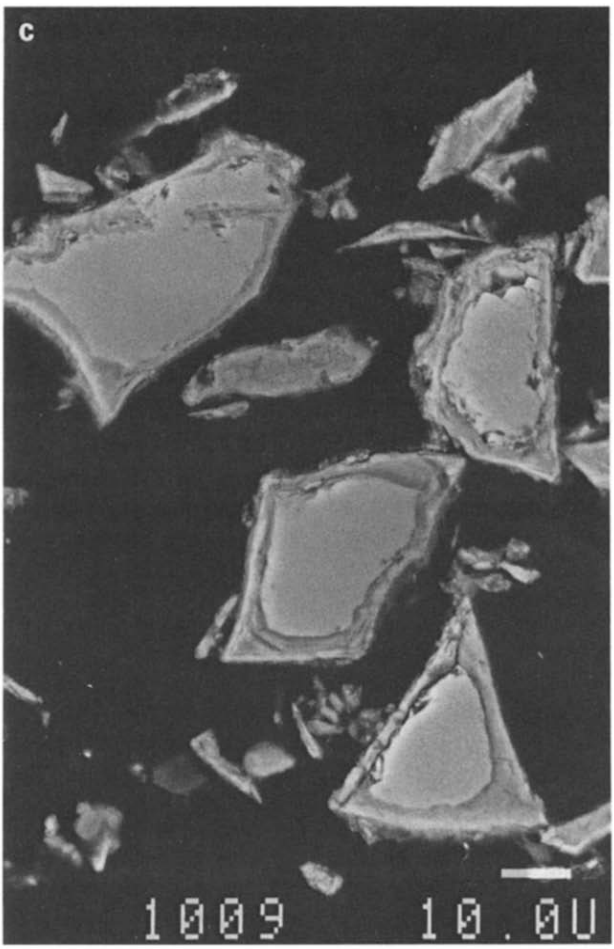

Fig. 2 (continued).

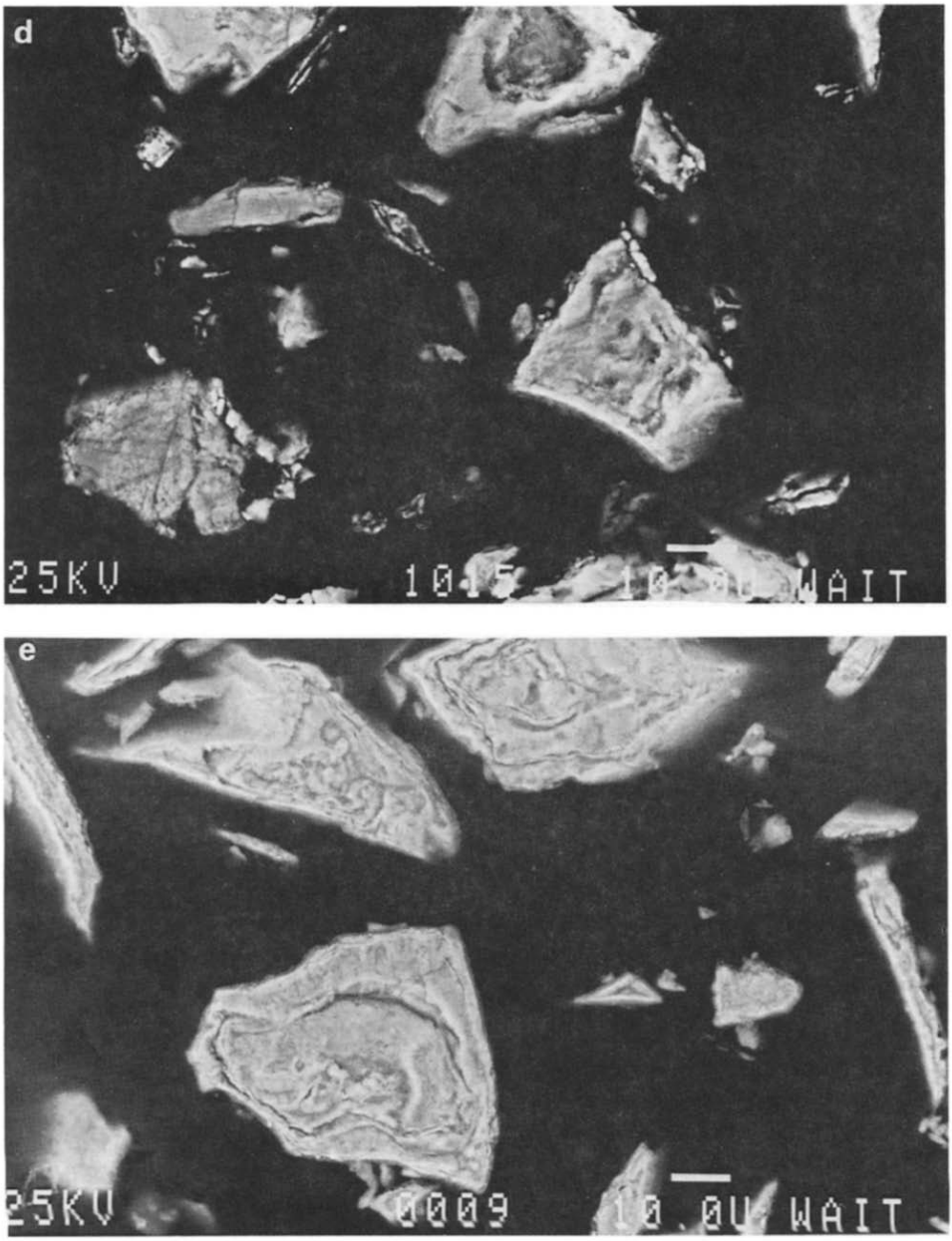

Fig. 2 (continued).

The partially reacted particles have a rim of what might be product phase of varying thickness surrounding what appears to be an unreacted core. The ratio of volume of unreacted core to the total volume, which is calculated assuming the particles to be ideal spheres, varied between 0 (for a completely reacted small particle) to 0.39 (for a partially reacted large particle).

The SEM micrographs of the particles heated to 505 °C and 696 °C are presented in Figs. 2d and e respectively. The particles appear to consist of rings of product material. There is no major distinction between the two sets of particles.

Iron and sulphur were determined quantitatively by X-ray analysis at certain points on a particle by use of the SEM in the spot mode. Particles of unreacted pyrite were used as internal standards. Each reacted particle was analysed at the rim and the centre. From these data the ratio of iron : sulphur was calculated and then the sulphur value normalised relative to iron.

Minor variations in the stoichiometric composition of unreacted pyrite particles were evident, although the iron : sulphur ratios were on average 1 : 2. However, the composition of a single particle appeared to be uniform as judged by the analysis at the rim and centre. The particles heated to 428 °C showed very little evidence of reaction, and the stoichiometry of the sulphide phase at the rim and centre was the same as the unreacted particles. By 470 °C, however, significant oxidation had occurred. As indicated in the SEM micrographs, not all the particles had reacted to the same extent. Some particles had reacted throughout, and had iron : sulphur ratios which were only slightly higher in sulphur at the centre than at the rim. These particles had compositions close to 1 : 1. In a few particles, the rim was almost completely oxidised and only a minor amount of sulphur was present. In contrast, the centre appeared to be unreacted, and gave an analysis which corresponded to pyrite. At 505 °C the samples were similar. However, for particles heated to 696 °C very little sulphur remained, indicating that complete reaction had occurred.

Combining the evidence from TG–DTA, XRD and SEM enables some comments to be made about reaction sequences and the temperature ranges over which they occur. Only minor reactions occurred below 390 °C. These presumably were either direct oxidation of pyrite to hematite or to $FeSO_4$, as previously found [1]. The formation of the latter compound is slow as indicated by isothermal TG studies [1]. Between 395 and 428 °C there are a number of sharp exotherms. Although the SEM results indicated no significant reaction by 428 °C, the quantitative XRD data indicated the presence of 6% hematite at this temperature. Consequently the sharp exotherms can be associated with the formation of this minor quantity of hematite. There is a deficit of 4% at this temperature, and although there is a large associated error in the estimation, it is an indication that some sulphate has formed.

The major oxidation reaction occurs between 420 and 490 °C, as indicated by the large exotherm in the DTA curve and the weight loss in the TG curve. Results from SEM and XRD confirmed that samples heated to 470 and 505 °C had undergone extensive reaction. By 470 °C 47% hematite was formed, and this increased to 65% by 505 °C. At the same time the quantity of phases unaccounted for increased to 17% and 25% at these two temperatures. If the formation of a ferric sulphate phase is assumed, then there are two possible routes.

(1) By oxidation of $FeSO_4$. This reaction has been shown to commence at 450 °C [3], followed by decomposition of $Fe_2(SO_4)_3$ above 550 °C. However the small quantity of $FeSO_4$ present at 428 °C as indicated by the XRD analysis (see Table 1) cannot account for the quantity of the ferric salt formed unless the rate of formation of the $FeSO_4$ suddenly increases. This seems unlikely, as other work has shown that $FeSO_4$ starts to decompose above 320 °C [1].

(2) By sulphation of hematite. An alternative reaction is for SO_2 to be oxidised to SO_3, followed by sulphation of the newly formed hematite. Platinum is known to catalyse the oxidation of SO_2 to SO_3.

This reaction sequence accounts for the two major reactions occurring in the same temperature range, as the oxidation of pyrite to hematite is a necessary prerequisite for the sulphation reaction.

By 505 °C, only 10% pyrite remained unreacted. We believe that the remainder of the sulphur is fixed in a ferric sulphate phase.

Although the quantitative SEM data collected at 470 °C showed Fe : S ratios near to pyrrhotite, the sulphur value determined is a composite of unreacted pyrite, sulphate and any other sulphide species such as pyrrhotite. It is not possible to calculate the values for the individual components, and hence establish the presence of pyrrhotite unequivocally. There is no evidence from XRD to support the existence of this phase, although it may be present below the detection limit. There is no evidence in the micrographs (Fig. 2) of the porosity found in particles when pyrrhotite is formed from the thermal decomposition of pyrite [4].

The SEM results indicate that oxidation of pyrite occurs by a shrinking core model. Thus oxidation commences at the surface and gradually penetrates towards the centre. At a heating rate of 2.5 °C min^{-1} the oxidation reaction occurred between approximately 400 and 500 °C. This 100 °C temperature interval equates to 40 min. Hence samples of ≈ 1.8 mg of particle size < 45 μm in a large excess of oxygen required at least 40 min from commencement to completion of reaction. This suggests that the oxide and sulphate layers formed on the surface of the particle are quite dense and provide a significant barrier to oxygen diffusion. The protective nature of sulphate layers during diffusion controlled oxidation has been demonstrated for manganese(II) sulphide [11].

The remaining 10% pyrite reacts above 505 °C, although there is no indication of exothermic effects above that temperature. However there is a slow weight loss between 480 and 550 °C which may be due to the continued slow oxidation of pyrite. It is also possible that interaction between pyrite and the sulphate phase occurs as previously suggested [5,6]. It is unlikely that any unreacted pyrite will exist above 550 °C, as the decomposition of pyrite to pyrrhotite occurs between 530 and 550 °C to produce vigorous exothermic reaction [4].

Above 550 °C the major reaction is the decomposition of the sulphate phase and the formation of more hematite.

Effect of heating rate

Figure 3 shows the effect of changing the heating rate from 2.5 to 40 °C min^{-1} on the TG–DTA curve for samples of pyrite in air.

The ratio of the first weight loss to the second is affected by the change in heating rate. It was found that the ratio increased with increase in heating rates. Consequently the slower heating rates favoured the formation of the sulphate phase. This is consistent with the known slow rate of sulphate formation through oxidation of pyrite.

An increase in heating rate is observed to shift mass losses to higher temperatures. The temperature at which the DTA peak commences is relatively constant, but the temperature at which the DTA curve returns to the baseline increases from about 490 to 550 °C. A decrease in the number of exothermic peaks is observed, especially the small sharp peaks which occur in the low temperature region of the major exothermic peaks. There is

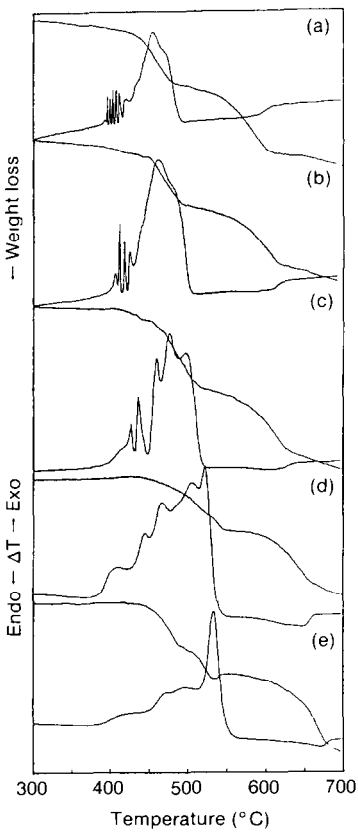

Fig. 3. TG–DTA traces of < 45 μm particles of pyrite heated at various rates in air. Heating rates (°C min^{-1}) and DTA sensitivities (μV) are as follows: (a) 2.5, 50; (b) 5, 100; (c) 10, 100; (d) 20, 200; (e) 40, 500.

also a tendency for the large exotherm which is complete by 490 °C at the slower heating rates to diminish in size and a new peak to appear between 500 and 550 °C. At 40 °C min^{-1} this peak is quite well resolved (Fig. 3e). This last trace was similar to those given in recent publications [4,8], with the major exotherm at 530–550 °C. At this fast heating rate the direct oxidation of pyrite to hematite may be too slow to be complete before a temperature is reached at which pyrite decomposes. This proposition will be examined in our next paper.

Effect of atmosphere

Figure 4 shows the effect of an oxygen atmosphere on the course of oxidation of pyrite of particle size < 45 μm.

Changing the atmosphere from air to oxygen causes a significant effect on the DTA record. At a heating rate of 2.5 °C min^{-1}, the DTA trace consists of a number of sharp, well resolved peaks in the temperature range

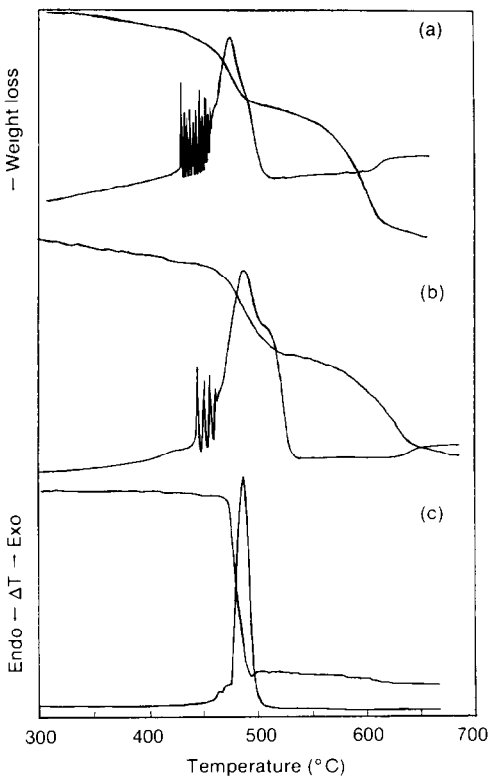

Fig. 4. TG–DTA traces of < 45 μm particles of pyrite heated at various rates in oxygen. Heating rates (°C min^{-1}) and DTA sensitivities (μV) are as follows: (a) 2.5, 50; (b) 10, 200; (c) 40, 500.

430–460 °C. After the sharp peaks there is a broad exotherm between 460 and 505 °C. Above this temperature is an endotherm. Increasing the heating rate to 10 °C min^{-1} decreases the number of sharp exothermic peaks, and shifts all peaks to higher temperatures.

At the fastest heating rate of 40 °C min^{-1} the DTA record undergoes a radical change. Apart from some minor peaks at around 470 °C (see Fig. 4c) only a single peak is apparent in the DTA curve. The peak is quite sharp and occurs over the temperature range 475–500 °C. This peak is also very intense, and comparison of values obtained in an air atmosphere at the same heating rate reveals that the peak in oxygen is four times greater than the corresponding peak in air. When the heating rate is monitored, there is significant distortion from linearity of the temperature in the range of the reaction. The temperature exceeds that expected from the programme, giving some indication of the heat generated by the reaction. The sample also glows red, whilst the furnace is still showing no red colouration. The associated weight loss occurs over a similar narrow temperature range. There is no evidence of the endothermic peak or second weight loss associated with the decomposition of sulphates.

Hematite is the only phase detected by XRD in this sample. Examination of reacted particles by SEM (see Fig. 5) indicates that they have a very high porosity, suggesting that the particles have been heated to at least 530–550 °C, which is the temperature at which pyrite decomposes to pyrrhotite. The increased porosity resulting from the decomposition of pyrite is well documented [12]. This overheating must arise from the initial exothermic reaction heating the particle above the TG–DTA furnace temperature, since the maximum temperature observed in the DTA record for the exotherm is 500 °C. The fast heating rate has also limited the oxide coating to a thin rim, thus giving less impedance to gas diffusion processes. The evolution of sulphur vapour outwards will be achieved rapidly as the activity of the sulphur increases at the decomposition temperature of pyrite, causing a rapid gas phase reaction between sulphur and oxygen to occur. This will induce further particle heating which will cause further reaction.

Although the fast heating rate mitigates against the formation of a ferric sulphate phase, nevertheless at 40 °C min^{-1} in air there was still a significant quantity formed as indicated by the magnitude of the second weight loss (Fig. 3e). Hence the absence of any second weight loss under similar conditions in oxygen is a further indicator that the samples have been heated above the furnace temperature. Since the second weight loss in air was not complete until approximately 680 °C, then the self-heating effect generated by the reaction was sufficient to raise the sample temperature to at least 680 °C. The decomposition of sulphate through heat generated during the oxidation of pyrite has been previously noted, although the oxidation occurred at higher temperatures and only when the sample was contained in a crucible of low conductivity [4].

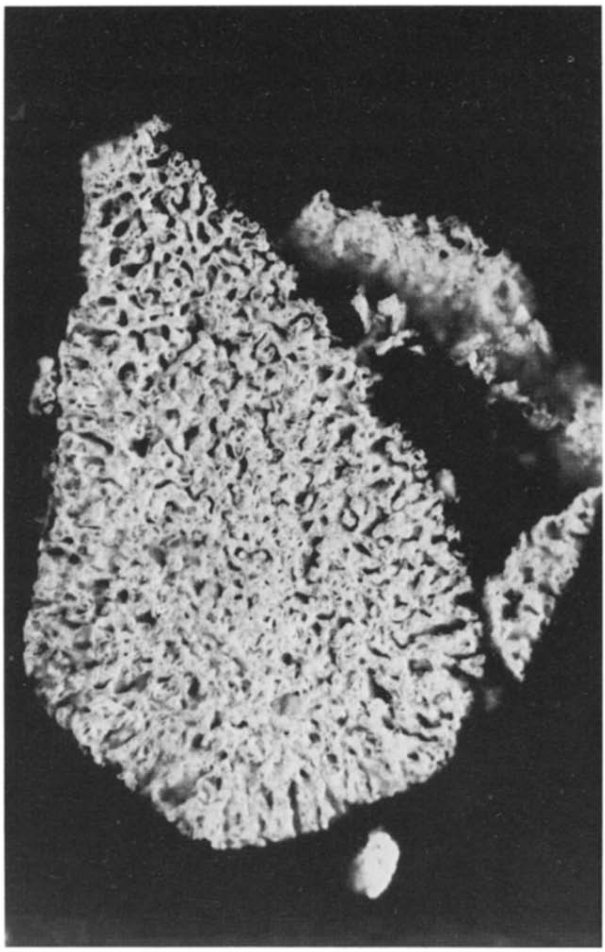

Fig. 5. Scanning electron micrograph of $< 45\ \mu m$ particles of pyrite heated at $40\,^{\circ}C\ min^{-1}$ in oxygen.

The properties of the TG–DTA trace obtained in oxygen at $40\,^{\circ}C\ min^{-1}$ taken in conjunction with the physical characteristics of the reacted particles suggest that these conditions ignite the pyrite particles rather than cause slow oxidation. By ignition we mean a process in which the heat generated by the oxidation of the sulphide is used to heat the particle rather than the surroundings. This self-heating effect causes the particle temperature to rise, which increases the rate of further oxidation, which generates more heat which raises the particle temperature further and so on. What ensues is a "runaway" reaction sequence that, as long as there is an excess of oxidant present, proceeds until reaction is complete. An ignition reaction is characterised by a single high energy emission that occurs in a narrow timespan and a particle temperature that increases rapidly and peaks well in excess of the furnace temperature [13]. Similar changes in reaction have been observed

when nickel sulphide concentrates have been heated rapidly in oxygen [13,14]. When faster heating rates were used, in the order of 4500 °C min^{-1}, pyrite could be ignited at temperatures as low as 390 °C [15].

CONCLUSIONS

On the evidence collected in this work, the formation of hematite from the oxidation of < 45 μm particles of pyrite in air and at a heating rate of 2.5 °C min^{-1} occurs primarily by direct oxidation of pyrite in the temperature range 420–490 °C. A ferric sulphate phase is formed simultaneously, which then decomposes between 550 and 610 °C to produce additional hematite. The reaction occurs via a shrinking core process, and the rate is controlled by oxygen diffusion. The coatings formed on the surface of the particles are protective, and the oxidation rate is slow.

Increasing the heating rate and the oxygen partial pressure has a significant effect on the appearance of the TG–DTA records. As the heating rate increased from 2.5 to 40 °C min^{-1} in air the number of peaks changed and shifted to different temperatures. These changes were too severe to be explained by changes in instrument parameters alone, and suggest that changes in reaction mechanism have occurred.

At the fastest heating rate studied of 40 °C min^{-1} in oxygen the DTA record is substantially different, and is attributed to a change in mechanism from a slow oxygen diffusion controlled reaction to an ignition reaction. This is the first time that this form of reaction has been reported for pyrite.

ACKNOWLEDGEMENTS

One of us (G.C.D.) thanks the People's Republic of Bangladesh and Jahangirnagar University for permission to pursue studies at Curtin University, and the Australian Development Assistance Bureau (ADAB) for financial support. We also thank Mr. I. Sills (Applied Chemistry) for technical assistance, Mr. A. Van Reissen (Applied Physics) for providing the SEM results, and Mr. L.C. Hammond and Mr. N. Kempt (Applied Physics) for measuring the XRD data.

REFERENCES

1 J.E. Pahlman and G.W. Reimers, Report of Investigations, 9059, U.S. Bureau of Mines, 1986.
2 J.R. Schorr and J.O. Everhart, J. Am. Ceram. Soc., 53 (1969) 351.
3 T. Kennedy and B.T. Sturman, J. Therm. Anal., 8 (1975) 329.

4 F.R.A. Jorgensen and F.J. Moyle, J. Therm. Anal., 25 (1982) 473.
5 A.C. Banerjee, P. Rangaswamy and S. Sood, in W. Hammenger (Ed.), Thermal Analysis, Vol. 2, ICTA 1980, Birkhaeuser, Basel, p. 241.
6 V.A. Luganov and V.I. Shabalin, Can. Met. Quart., 21 (1982) 157.
7 F. Paulik, J. Paulik and M. Arnold, J. Therm. Anal., 25 (1982) 313.
8 C.M. Earnest, Thermochim. Acta, 75 (1984) 219.
9 F.R.A. Jorgensen and F.J. Moyle, Metall. Trans. B, 12 (1981) 769.
10 B.H. O'Connor and J. Jaklevic, X-Ray Spectrosc., 9 (1980) 60.
11 T.R. Ingraham and P. Mauriar, Trans. Met. Soc. AIME, 242 (1968) 2039.
12 F.J. Arriagada and K. Osseo-Asare, Precious metals: mining, extraction and processing, in V. Kudryk, D.A. Corrigan and W.W. Liang (Eds.), Am. Inst. Min., Metall. and Pet. Eng., Inst. Met. Div., Spec. Rep. Ser., 1984, p. 367.
13 J.G. Dunn, S.A.A. Jayaweera and S.G. Davies, Proc. Australas. Inst. Min. Metall., 290 (1985) 75.
14 J.G. Dunn and S.A.A. Jayaweera, Thermochim. Acta, 61 (1983) 313.
15 J.G. Dunn, S.G. Davies and L.C. Mackey, Proc. Australas. Inst. Min. Metall., in press.